

## Depolarization experiments on space charges in concentrated solid solutions of $\text{NdF}_3$ in $\text{SrF}_2$

J. Meuldijk, H. H. Mulder, and H. W. den Hartog

*Solid State Physics Laboratory, 1 Melkweg, 9718 EP Groningen, The Netherlands*

(Received 10 November 1981)

The influence of the defect concentration on the relaxation of space charges in  $\text{Sr}_{1-x}\text{Nd}_x\text{F}_{2+x}$  solid solutions has been investigated with the ionic-thermocurrent technique. A concentration domain of 0.004 up to 45 mol % has been used. As in the system  $\text{Ba}_{1-x}\text{La}_x\text{F}_{2+x}$  the space-charge relaxation band (high-temperature band) shifts to lower temperatures with increasing  $\text{RF}_3$  concentration. A percolation model has been used to explain these shifts. Most of the differences between the systems  $\text{Sr}_{1-x}\text{Nd}_x\text{F}_{2+x}$  and  $\text{Ba}_{1-x}\text{La}_x\text{F}_{2+x}$  are reducible to different dipolelike jumps supporting the charge transport: nearest-neighbor dipolelike jumps in  $\text{Sr}_{1-x}\text{Nd}_x\text{F}_{2+x}$  and next-nearest-neighbor dipolelike jumps in  $\text{Ba}_{1-x}\text{La}_x\text{F}_{2+x}$ . The charge transport may be interpreted qualitatively with a percolation mechanism.

### I. INTRODUCTION

Alkaline-earth fluorides doped with small amounts of trivalent impurities have been investigated in detail by means of various techniques in the recent literature.<sup>1-15</sup> Electron paramagnetic resonance (EPR) and electron-nuclear double resonance (ENDOR) have played an important role in the determination of the kind of impurities present in these materials.<sup>16-19</sup> From these experiments we know that in rare-earth-doped samples there are three different kinds of centers: In some cases there are cubic impurities, which suggests that the excess charge of the trivalent ions has been compensated nonlocally; in other samples one finds permanent electric dipoles consisting of a trivalent impurity and a nearby interstitial fluoride ion ( $R^{3+}\text{-F}_i^-$  dipoles). If we consider the lattice structure of the alkaline-earth fluoride crystal, we see that one may choose the position of the interstitial  $\text{F}^-$  ion in any of the successive coordination shells of the central  $R^{3+}$  impurity.

The experimental facts published until now show unambiguously that in some crystals the interstitial  $\text{F}^-$  ion is located in the first coordination shell of interstitial sites [nearest-neighbor (NN) dipoles]; in other samples the interstitial is found in the second shell of interstitial sites [next-nearest-neighbor (NNN) dipoles]. The schematic representation of the two different dipoles has been given in Fig. 1.

Ionic-thermocurrent (ITC) experiments per-

formed in our laboratory have shown that in order to be able to derive the important parameters  $E$  and  $\tau_0$  from the depolarization peaks, using the formula given by Bucci *et al.*,<sup>20</sup> it is necessary to work with samples doped with very small concentrations of  $R^{3+}$  ions.<sup>8</sup> In samples with moderate concentrations of trivalent ions (0.01–0.1 mol %) we have found ITC peaks which could not be described anymore with the simple Bucci and Fieschi formula; therefore, van Weperen *et al.*<sup>9</sup> derived a new formula in which they have taken into account the interaction between the defects. If the concentration is increased further, not only the jump processes, which appear to be very sensitive

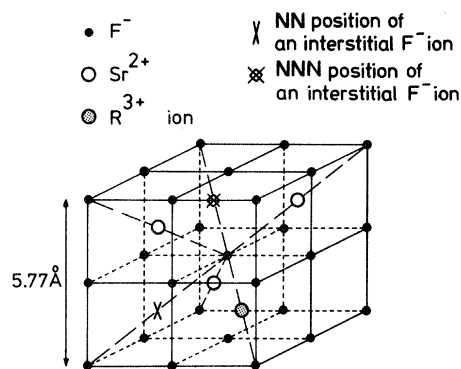


FIG. 1. Three-dimensional schematic representation of an  $\text{SrF}_2$  crystal showing the structure of a tetragonal (NN) and a trigonal (NNN)  $R^{3+}\text{-F}_i^-$  complex.

to variations of the concentration, but also the defect structure are affected by the defect-defect interactions as shown by Aalbers and den Hartog.<sup>21</sup>

On the other hand, some authors have found that for  $RF_3$  concentrations higher than 0.1 mol %, clustering of the impurities occurs.<sup>22-25</sup> The present experimental results suggest that clustering takes place only for specific  $R^{3+}$  dopants; it is probable that it is not a phenomenon which is common to all rare-earth impurities. ITC can also be employed to study the effects of clustering of dipoles. This has been done for various systems of the type  $XF_2:R^{3+}$  ( $X = Ca, Sr, \text{ or } Ba$ ) in our laboratory.<sup>26</sup>

In this paper we present new ITC results on  $SrF_2$  samples doped with  $NdF_3$ . Samples with Nd concentrations up to 45 mol % have been investigated. Crystals with impurity concentrations in this range have the fluorite structure. It turns out that in crystals with about 8 mol %  $NdF_3$  we can observe a very weak ITC peak due to the reorientation of NN dipoles. For higher concentrations this band is no longer observable because of the presence of a very intense ITC peak close to the NN dipole peak. Apart from the NN dipole band we observed in  $SrF_2:Nd$  another depolarization peak, which is usually located at rather high temperatures (the HT peak). The most remarkable properties of the HT peak are the very high intensity and the varying position as a function of the Nd concentration. With regard to the latter property we found that for very low concentrations the temperature corresponding with the maximum depolarization current approaches a maximum value. For very high concentrations the HT band is located at a position close to that of the NN dipole peak. Also the width of the HT band as a function of the Nd concentration has been investigated.

We have found that both the position of the space-charge depolarization (HT) band and the variations of the width with the Nd concentration can be understood by applying the model that has been proposed by den Hartog and Langevoort.<sup>27</sup> According to this model the depolarization of the crystal is described by a relaxation mechanism, which consists of two different jumps: (a) the jumps of free interstitial fluoride ions, and (b) jumps of fluoride ions in NN dipole complexes. With increasing Nd concentration the relative contribution of the NN dipole jump mechanism increases, leading to a decrease of  $T_{max}$  (the temperature for which the depolarization current reaches its maximum value).

It appears that, just as we did for the system  $BaF_2:La$ , we can, for high Nd impurity concentrations, consider the sample to consist of two regions: (a) the high-conductivity regions formed by the reorienting dipolar complexes, and (b) the pure  $SrF_2$  in which the ionic conductivity is very low. In this paper we employ this model in order to understand the depolarization effects due to space charges and the ionic conductivity of heavily doped fluorite-type crystals. We find that the ionic conductivity in these materials can be described roughly in terms of a percolation mechanism similar to the one treated by Kirkpatrick.<sup>28</sup> The critical concentration for percolation-type conduction is about 10 mol % for the system  $SrF_2:Nd$ , which suggests that dipolelike jumps contribute to the conduction. This should be compared with the value of 2.2 mol % found for  $Ba_{1-x}La_xF_{2+x}$ , where the conduction is due to the NNN instead of NN dipole jumps. The former dipole systems have a much larger volume than the latter ones, leading to a much smaller critical concentration for  $Ba_{1-x}La_xF_{2+x}$ . For concentrations higher than the critical one the conductivity increases very rapidly with the concentration.

## II. EXPERIMENTAL PROCEDURES

The single crystals used for this investigation have been prepared in a high-frequency crystal-growing setup. The method employed is a modified Bridgman technique; we have used highly pure carbon crucibles with an inner diameter of 8 mm. In general, we have grown our crystals from  $SrF_2$  (Merck, Suprapur) and  $NdF_3$  (Ventron, 99.9% pure). In order to reduce the  $O^{2-}$  and  $OH^-$  content of the crystalline material we added approximately 2 mol %  $PbF_2$  (Koch-Light, 99.95% pure) before crystal growth. The growth rate of the machine can be chosen in the interval 0.5–20 mm/h; for our crystals we have adjusted the growth rate at about 6 mm/h. After the crystals (in our setup we are able to prepare seven crystals at the same time) have been removed from the hot zone, the temperature of the crystals is decreased further very slowly by reducing the high-frequency power; after about 15–20 h room temperature is reached.

In this investigation we employed cylindrical samples, cut from the as-grown crystal boules by means of a slide wire saw; the diameter is 8 mm, the thickness is between 1.5 and 2.0 mm. Before the samples are placed in the ITC setup the sur-

faces are polished very carefully; special attention has been paid to carbon and other impurities, which may cause conduction between the electrodes. The samples are covered with a thin foil of teflon; the electrodes are pressed onto the circular faces of the sample and are kept in that way by means of a spring. The polarizing voltage across the sample is usually 4 kV; this voltage is applied at temperatures well above the temperature corresponding with the maximum depolarization current ( $T_{\max}$ ). The influence of the variation of the polarizing field has been examined and no changes of the peak positions or peak widths were found. In our setup at  $T_{\max}$  the relaxation time is about 100 sec, implying that it is sufficient to polarize the sample during a few minutes. After the polarization phase the cooling phase takes about 20 min; during this period of time the temperature is decreased until it is well below the position of the NN dipole peak ( $\sim 150$  K). After one or two hours the depolarization phase is started by heating the sample linearly with time at a rate of about  $0.03 \text{ K sec}^{-1}$  until a maximum temperature of 340–370 K is reached.

The EPR experiments have been performed with Varian spectrometers ( $Q$  and  $X$  band) operating at 35 and 9.2 GHz, respectively. The experiments were carried out with samples containing cubic, tetragonal, and trigonal  $\text{Gd}^{3+}$  impurities. The linewidths of the different fine lines of the EPR signal of cubic  $\text{Gd}^{3+}$  have been determined. Extra attention has been paid to the transitions  $S_z = \frac{5}{2} \leftrightarrow \frac{7}{2}$ ,  $\frac{3}{2} \leftrightarrow \frac{5}{2}$ ,  $\frac{1}{2} \leftrightarrow \frac{3}{2}$ ,  $-\frac{3}{2} \leftrightarrow -\frac{1}{2}$ ,  $-\frac{5}{2} \leftrightarrow -\frac{3}{2}$ , and  $-\frac{7}{2} \leftrightarrow -\frac{5}{2}$ ; the transition  $S_z = -\frac{7}{2} \leftrightarrow -\frac{5}{2}$  is, as expected, not very sensitive for perturbations from distant point charges or dipoles.

The concentrations of the  $\text{Nd}^{3+}$  impurities in the samples have been determined by means of x-ray fluorescence. It turned out that in some cases there are appreciable variations of the  $\text{Nd}^{3+}$  concentration in the crystal boule. We have therefore determined the  $\text{Nd}^{3+}$  concentrations for all ITC samples investigated in this paper. In order to guarantee reproducible geometry and correct values for the concentration ( $x$ ) we have crushed the samples and pressed pills from the resulting powder. Below 1 mol % the sensitivity of this method for the system  $\text{Sr}_{1-x}\text{Nd}_x\text{F}_{2+x}$  is too low to get reliable results. Therefore, below 1 mol % weighted-in values are taken for the concentration.

Another way to approximately determine the concentration of  $\text{Nd}^{3+}$  in the samples is the optical-absorption method. The Nd-doped  $\text{SrF}_2$

crystals are slightly colored; consequently there is an absorption in the visible part of the spectrum. The absorption bands observed are rather narrow, and therefore this technique is quite sensitive. This method has been used mainly to get an idea about the concentration very quickly.

### III. EXPERIMENTAL RESULTS

In  $\text{SrF}_2$  crystals, which are doped with small concentrations of  $\text{NdF}_3$ , we only find NN dipoles. This is in agreement with the results obtained by Lenting *et al.*,<sup>8</sup> who also observed for low-impurity concentrations that the first elements of the lanthanide series only give rise to NN dipoles, whereas for the heavy rare-earth ions only NNN dipoles can be observed. The two different dipoles can easily be distinguished because the NN dipoles cause an ITC peak at about 150–155 K, while NNN complexes give a dipole-reorientation peak at about 210 K (see Lenting *et al.*<sup>8</sup>). It has been found by our group that the positions of the two dipole peaks are only slightly rare-earth dependent.<sup>8,10</sup>

Apart from the dipole-reorientation peaks we have found a very intense ITC band, which is usually located at rather high temperatures ( $T > 300$  K). The intensity of this band is so large that it is very difficult to explain it in terms of dipole-reorientation processes. We would need dipole strengths of at least 3–5 times as large as that of the NNN dipole, which is already  $5.0e \text{ \AA}$  (see Aalbers and den Hartog<sup>21</sup>), in order to explain the total displaced charge during the polarization process.

In Fig. 2 we show a survey of the ITC results of a  $\text{SrF}_2$  crystal doped with 0.07 mol %  $\text{NdF}_3$ . We observe a weak band at low temperatures ( $\sim 150$  K) and a very strong one at about 350 K. In the following we refer to these bands as the low-temperature (LT) and the high-temperature (HT) band, respectively.

We have found that for  $x \leq 10^{-2}$  the LT band increases in intensity if we add more  $\text{NdF}_3$  to our crystals; the position of the band remains unchanged. This is in agreement with the observation made by den Hartog and Langevoort,<sup>27</sup> who reported that in crystals  $\text{BaF}_2:\text{La}$  and  $\text{SrF}_2:\text{La}$  the dipole-reorientation bands have a fixed position. The HT peak, however, varies drastically as a function of the Nd concentration. For very low Nd concentrations it is located at 345–350 K; in cubic crystals doped with 45 mol %  $\text{NdF}_3$  this

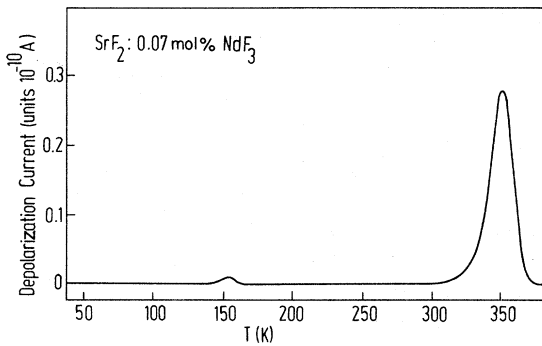


FIG. 2. Example of a complete ITC run of  $\text{SrF}_2$  containing 0.07 mol %  $\text{NdF}_3$ .

peak is found at 156 K. We note that this temperature is lower than the fixed position of the NNN dipole peak in  $\text{SrF}_2$  (see Lenting *et al.*<sup>8</sup> and van Weperen and den Hartog<sup>10</sup>).

A survey of the results of the HT-peak positions as a function of the Nd concentration has been presented in Fig. 3, where it can be seen that for concentrations below 0.1 mol % the position of the HT peak does not vary significantly. In the concentration range 1–45 mol % the HT peak shifts to lower temperatures as a function of the Nd concentration very rapidly. An important feature of our experimental results is also that the width of the HT band is constant for low Nd concentrations (<0.5 mol %); for higher concentrations it increases, reaches a maximum value at about 5 mol % and it decreases again with the concentration in the range  $0.05 < x < 0.45$  (see Fig. 4). In order to demonstrate this effect, we show in Fig. 5 three ITC curves with the HT and, eventually, the

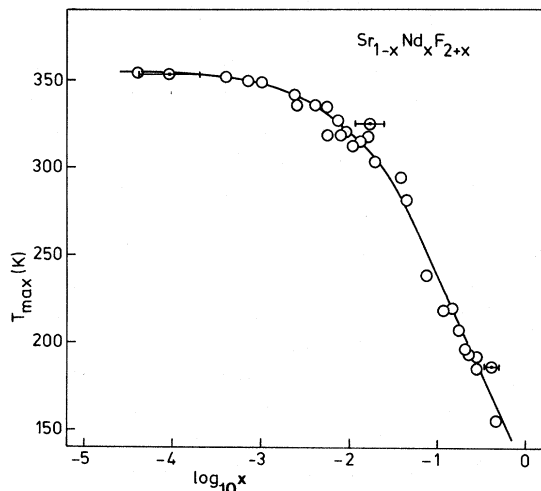


FIG. 3. Experimentally determined HT band position as a function of  $\log_{10} x$  for  $\text{Sr}_{1-x}\text{Nd}_x\text{F}_{2+x}$ .

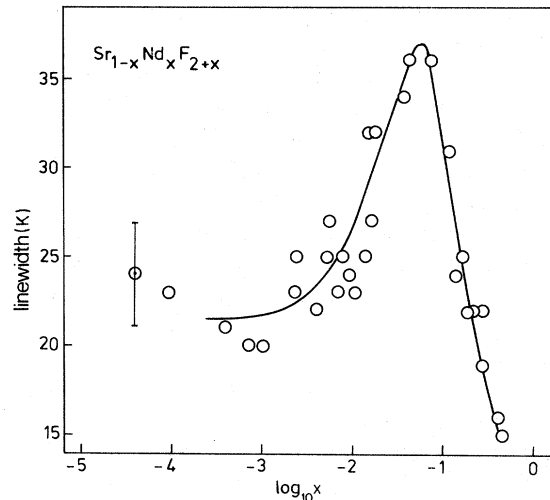


FIG. 4. Experimentally determined HT bandwidth at half height as a function of  $\log_{10} x$  for  $\text{Sr}_{1-x}\text{Nd}_x\text{F}_{2+x}$ .

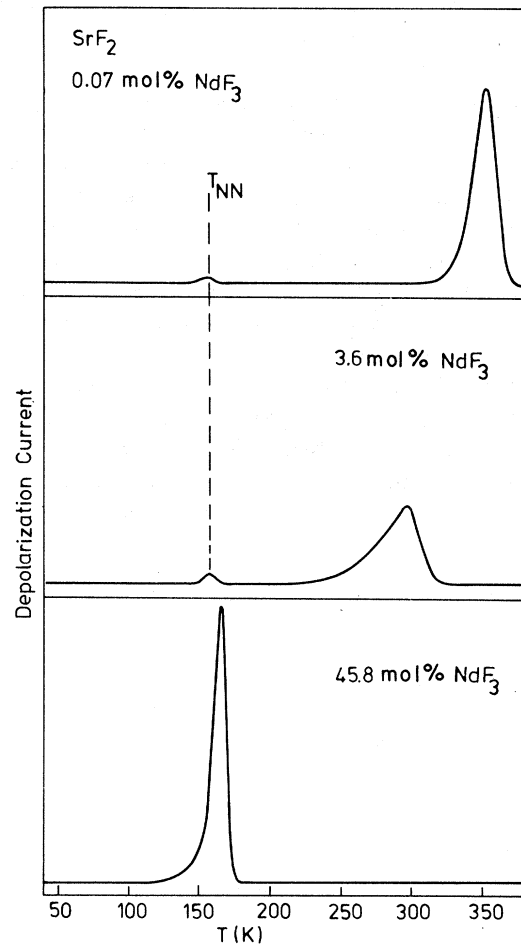


FIG. 5. Survey of the ITC results for  $\text{SrF}_2:\text{Nd}$  crystals in the concentration range 0.07–45.8 mol %.

LT band. Also, from Fig. 5, the dramatic shifts of the HT band can be observed and we can see that even for large Nd concentrations (such as 3.6 mol %), dipoles of the NN type are still present.

In Fig. 6 the intensity of the LT peak has been plotted as a function of the  $\text{NdF}_3$  concentration. It appears that up to 1 mol %  $\text{NdF}_3$  the intensity of the LT peak increases with increasing concentration of Nd impurities. For higher concentrations the dipole-reorientation peak decreases rapidly with the Nd content, indicating that in samples heavily doped with Nd at least part of the impurities are present in positions different from the well-known NN charge-compensation sites. There are now several possibilities. The first one is that instead of NN dipoles at high concentrations NNN complexes are formed. The second one is that due to clustering of the dipolar defects the formation of simple charge-compensation centers is reduced. The third one is that we may propose that at high concentrations nonlocal charge compensation (i.e., the formation of cubic  $\text{Nd}^{3+}$ ) becomes more favorable.

We have carried out experiments to obtain evidence for one of the possibilities mentioned above. From our experimental results reviewed above we note that there is no trace of a dipole peak associated with NNN complexes. In order to be completely certain about this we checked all samples in the concentration range  $0 < x < 0.04$  very carefully.

In  $\text{SrF}_2$  samples doped with both Nd and a trace of Gd an ITC peak due to NNN dipoles has been observed. These dipoles are  $\text{Gd}^{3+} - \text{F}_i^-$  charge compensators. This has been proven with EPR ( $X$  and  $Q$  band) measurements. The concentration of these NNN dipoles behaves in a rather peculiar way. At very low Nd concentrations the ITC peak

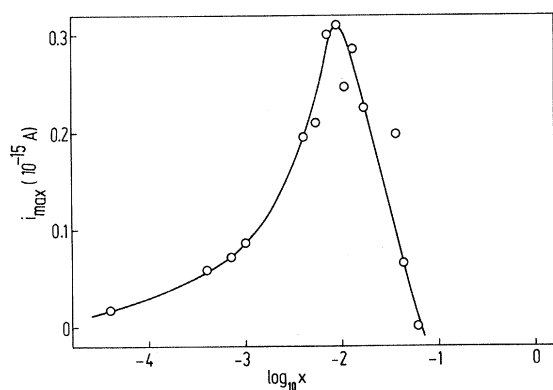


FIG. 6. LT-peak intensity for  $\text{Sr}_{1-x}\text{Nd}_x\text{F}_{2+x}$  samples as a function of  $\log_{10} x$ .

associated with NNN dipoles is relatively large; with increasing Nd concentration this peak decreases very rapidly, and at a concentration of 0.1 mol % the NNN peak due to  $\text{Gd}^{3+} - \text{F}_i^-$  centers has disappeared completely. Similar behavior has been observed in EPR; for low Nd concentrations all  $\text{Gd}^{3+}$  is present in the form of  $\text{Gd}^{3+} - \text{F}_i^-$  complexes (NN or NNN), whereas above a certain Nd concentration the  $\text{Gd}^{3+}$  ions are predominantly located at unperturbed cubic sites. It should be noted that similar behavior has been observed in samples doped with  $\text{Gd}^{3+}$  and  $\text{La}^{3+}$  (Ref. 29) and in samples doped with both  $\text{Gd}^{3+}$  and  $\text{Ce}^{3+}$ .<sup>30-32</sup> It appears that in  $\text{SrF}_2$  crystals  $\text{Gd}^{3+}$  impurities are located predominantly at cubic sites if there are sufficient trivalent impurities with a large ionic radius.

We have also checked the possibility of clustering in heavily doped crystals. Because it is impossible to measure EPR spectra at the corresponding Nd concentrations, we have employed  $\text{Gd}^{3+}$  probes to observe eventual clusters by means of EPR. In this way we can observe clusters containing a  $\text{Gd}^{3+}$  ion, if present in sufficient concentrations. However, referring to the experimental results given above, we should realize that  $\text{Nd}^{3+}$  and  $\text{Gd}^{3+}$  behave differently in  $\text{SrF}_2$ . Thus, it is not certain whether it is possible to exchange  $\text{Nd}^{3+}$  in clusters by  $\text{Gd}^{3+}$ . We have investigated  $\text{SrF}_2:\text{Nd}$  samples containing  $\text{Gd}^{3+}$  probes for Nd concentrations up to 6 mol % and we did not find any evidence for the formation of clusters containing  $\text{Gd}^{3+}$  impurities. We observed that the  $\text{Gd}^{3+}$  impurities are located at cubic sites; the only effect of the  $\text{Nd}^{3+}$  impurities on the EPR spectra is a drastic broadening of the individual resonance lines. This broadening can be understood if we take into account the electrostatic interactions between the central  $\text{Gd}^{3+}$  electrostatic interactions between the central  $\text{Gd}^{3+}4f^7$  electron system and the surrounding effective positive and negative charges associated with the  $\text{Nd}^{3+}$  ions and the interstitial  $\text{F}^-$  ions.<sup>33</sup>

In an earlier paper (Aalbers and den Hartog<sup>21</sup>) we have investigated the defect structure of the system  $\text{SrF}_2:\text{Gd}^{3+}$  as a function of the Gd concentration. We observed that as a result of the defect-defect interactions the formation of NNN dipoles is enhanced at concentrations higher than  $10^{18} \text{ cm}^{-3}$ . In the present case similar effects may play a role leading to the formation of an increased number of cubic  $\text{Nd}^{3+}$  impurities. It should be noted that probably the defect-defect interactions in a crystal containing cubic  $\text{Nd}^{3+}$  and interstitial

$F^-$  ions are significantly stronger than in a crystal containing dipolar complexes (NN or NNN). This leads to an appreciable broadening of the energies associated with the various defects present. If the mean energies of the different possible  $Nd^{3+}$  centers are very close to each other ( $\Delta E \sim 5.10^{-2}$  eV), significant variations of the defect structure are expected to occur as a function of the impurity content. Cubic  $Nd^{3+}$  may become an especially important defect because the energy of this effect is broadened very strongly as a result of the strong monopole-monopole and monopole-dipole interactions. In Table I we have compiled the most important results obtained for the HT peak of the complete series of  $SrF_2:Nd$  samples investigated in this work.

#### IV. THEORY

den Hartog and Langevoort<sup>27</sup> have investigated crystals of the types  $SrF_2:La$  and  $BaF_2:La$ . Their results indicate that for heavily doped crystals the ionic conduction is governed by dipolelike jumps of interstitial fluoride ions. As we have found in earlier investigations that the type of dipoles present in fluorite-type crystals depends upon the radius of the trivalent dopant ions, it is of interest to find out which dipolelike jumps take place in heavily doped crystals.

In  $SrF_2:La$  and  $BaF_2:La$  we have observed that the important jump parameters associated with the HT (ionic-conductivity) peak are very similar to those of the NNN dipole jumps. We therefore concluded that at high La concentrations the conduction process proceeds via NNN-type jumps of interstitial fluoride ions. It should be noted here that at low La concentrations only NN dipoles are present in  $SrF_2$ , whereas in  $BaF_2$  there are NNN-type dipoles. At high concentrations the NNN dipole reorientation peak develops in  $SrF_2$  and this makes the above-mentioned conduction process possible.

In  $SrF_2:Nd$  crystals only NN dipole jumps have been detected with ITC; we have investigated very carefully whether or not NNN dipoles are formed at high Nd concentrations. In Sec. III we have shown that this is not the case. Therefore, we may expect that NNN dipolar jumps do not play an important role in the conduction process of  $SrF_2$  heavily doped with  $NdF_3$ . If this is true, then the HT peak will show here a different behavior as a function of the concentration of the trivalent impurities as compared to that observed for the sys-

TABLE I.  $NdF_3$  concentrations, HT band positions, and HT band widths at half height for  $Sr_{1-x}Nd_xF_{2+x}$  samples investigated.

Concentration mol %	$T_{max}$ (K)	Linewidth (K)
45.8	156.0	15
40.5	187.3	16
29.4	185.9	19
26.6	192.7	22
22.6	193.0	22
20.4	197.2	22
16.8	207.8	25
14.5	220.9	24
11.6	218.2	31
7.5	239.1	36
4.3	281.9	36
3.6	295.2	34
1.80	303.3	32
1.65	325.9	32
1.62	318.9	27
1.30	315.2	25
1.08	313.6	23
0.90	320.7	24
0.79	318.6	25
0.70	327.0	23
0.55	319.0	27
0.54	334.6	25
0.40	336.7	22
0.24	336.1	25
0.23	342.1	23
0.10	349.2	20
0.07	349.2	20
0.04	352.0	21
0.009	352.8	23
0.004	354.3	24

tems  $SrF_2:La$  and  $BaF_2:La$ . In  $SrF_2:Nd$ , and also for strongly doped materials, NN-type jumps will be dominant. This has several consequences as will be indicated below.

den Hartog and Langevoort<sup>27</sup> have shown that heavily doped samples can be described by means of a model material consisting of an insulating host in which conducting spheres have been embedded. The size of these spheres should be taken equal to that of the sphere of a reorienting dipole system. For an NNN dipole this volume is about 11 times the volume of an alkaline-earth fluoride molecule. We have applied the usual percolation formula for the conductivity

$$\sigma = A(x - x_c)^{1.8}, \quad (1)$$

where  $x_c$  is a critical concentration. Above this

concentration the conductivity increases very rapidly as a function of the concentration  $x$ . We note that in Eq. (1) we have used the "mole fraction" as the parameter  $x$ , whereas in the current literature on percolation mechanism most authors use volume fractions. It is easy to transform Eq. (1) if one multiplies  $x$  and  $x_c$  by a factor of 11 in the case of NNN dipoles and by 2 for NN dipoles. Because the critical volume fractions are in cubic material between 25% and 30% one expects for  $x_c$  a value of 2–3 mol % if one is dealing with NNN dipole jumps and 10–15 mol % for NN-type jumps. From the result for NN dipoles we expect that it is possible to also observe percolation currents due to NN-type jumps in very heavily doped materials, because we have prepared cubic-solid solutions of SrF<sub>2</sub> and NdF<sub>3</sub> with Nd concentrations up to 45 mol %.

The large difference between the critical concentrations for crystals containing NNN and NN di-

poles is due to the difference in size of the reorienting dipole spheres. At relatively low  $R^{3+}$  concentrations the spheres of NNN dipoles tend to overlap; this is not the case for the smaller NN dipoles.

In order to test the percolation model for the conductivity in SrF<sub>2</sub>:Nd we have calculated the position of the HT peak on the basis of an ITC relaxation mechanism which can be described by the formula:

$$\frac{1}{\tau} = \frac{(1-\alpha)}{\tau_{\text{free interstitials}}} + \frac{\alpha}{\tau_{\text{NN dipoles}}} \quad (2)$$

The form of the ITC peak can be calculated in a straightforward way (see den Hartog and Langevoort<sup>27</sup>). Also, the maximum value of the ITC curve ( $T_{\text{max}}$ ) can be calculated rather easily for this mechanism. We have derived the following relationship:

$$(T_{\text{max}})^2 = \frac{b \left[ \frac{(1-\alpha)E_0^f}{\tau_0^f k} \exp\left(\frac{-E_0^f}{k_B T_{\text{max}}}\right) + \frac{\alpha E_0^d}{\tau_0^d k} \exp\left(\frac{-E_0^d}{k_B T_{\text{max}}}\right) \right]}{\frac{(1-\alpha)}{\tau_0^f} \exp\left(\frac{-E_0^f}{k_B T_{\text{max}}}\right) + \frac{\alpha}{\tau_0^d} \exp\left(\frac{-E_0^d}{k_B T_{\text{max}}}\right)} \quad (3)$$

We take for the parameters  $b = 0.03 \text{ K sec}^{-1}$  (= heating rate during the ITC experiment),  $\tau_0^f = 1.12 \times 10^{-11} \text{ sec}$ ,  $E_0^f = 0.94 \text{ eV}$ ,<sup>1</sup>  $\tau_0^d = 2.3 \times 10^{-14} \text{ sec}$ , and  $E_0^d = 0.47 \text{ eV}$ . The last values  $\tau_0^d$  and  $E_0^d$  were calculated from the LT peak of the sample with 0.03 mol % NdF<sub>3</sub> with our computer program which fits ITC peaks originating from dipole reorientations.<sup>9</sup> We can now calculate the values of  $T_{\text{max}}$  as a function of  $\alpha$ . With the values of  $\tau_0^f$  and  $E_0^f$  (and  $\alpha=0$ ) mentioned above we do not get a linewidth which is in agreement with the linewidth found experimentally for samples with a very low NdF<sub>3</sub> concentration. A better combination of parameters, giving the proper value of  $T_{\text{max}}$ , is  $\tau_0^f = 9.6 \times 10^{-15} \text{ sec}$  and  $E_0^f = 1.16 \text{ eV}$ . The origin of the difference between these relaxation parameters for the free-interstitial jumps and  $\tau_0^f$  derived from the Bollman activation energy of 0.94 eV (Ref. 1) and from the position of the HT peak at very low NdF<sub>3</sub> concentrations may be explained by association of the interstitial fluoride ions with impurities other than NdF<sub>3</sub> which are always present in very small amounts. In our ITC experiments these associations may be

considerable while in the conduction experiments<sup>1</sup> complete dissociation occurs because in the latter experiments the temperatures are 100–300 K higher than in our ITC experiments. The results of the calculations,  $T_{\text{max}}$  and the linewidth as a function of  $\log_{10}\alpha$ , have been displayed in Figs. 7 and 8, respectively. Figure 7 shows that for small values of  $\alpha$  the value of  $T_{\text{max}}$  is constant and equal to the value obtained for SrF<sub>2</sub> crystals containing a very small amount of NdF<sub>3</sub> (concentrations smaller than  $10^{-2} \text{ mol } \%$ ). For values of  $\alpha$  greater than  $2-3 \times 10^{-10}$ ,  $T_{\text{max}}$  decreases rather quickly as a function of  $\alpha$ .

Defining  $\alpha$  as the probability of placing a free-interstitial fluoride ion in the neighborhood of a cubic Nd<sup>3+</sup> ion forming an NN dipole,<sup>27</sup> we can translate  $\alpha$  in terms of the concentration of free-interstitial fluoride ions and cubic Nd<sup>3+</sup> ions. In the neighborhood of such a cubic Nd<sup>3+</sup> there are six interstitial positions. If one of these positions is occupied by a fluoride ion an NN dipole is formed. In dilute solutions we may approximate  $\alpha$  by  $6c_{\text{Nd}^{3+}(\text{cubic})}$ . As the concentrations of the free interstitials and the cubic Nd<sup>3+</sup> ions are approxi-

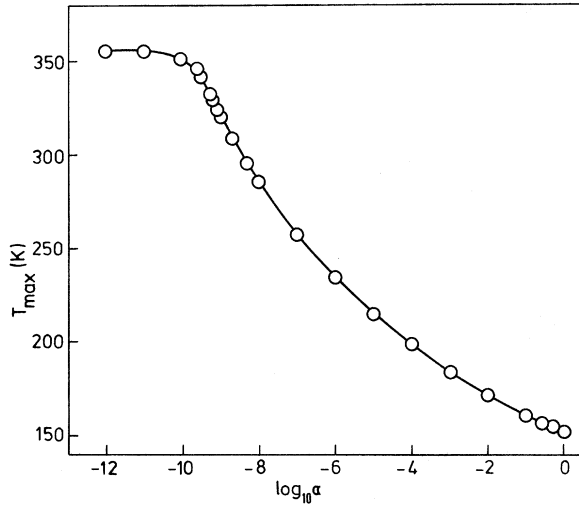


FIG. 7. Calculated HT-band position as a function of  $\log_{10}\alpha$ . The parameters used are  $E_0^f = 1.16$  eV,  $\tau_0^f = 9.6 \times 10^{-15}$  sec,  $E_0^d = 0.47$  eV,  $\tau_0^d = 2.3 \times 10^{-14}$  sec, and  $b = 0.03$  K sec $^{-1}$  (= heating rate during the ITC experiment).

mately equal and the  $\text{Nd}^{3+}$  ions are at fixed positions in the lattice, we can define the dissociation constant of NN dipoles as follows:

$$K_{\text{diss}} = \frac{\alpha}{6x} \quad (4)$$

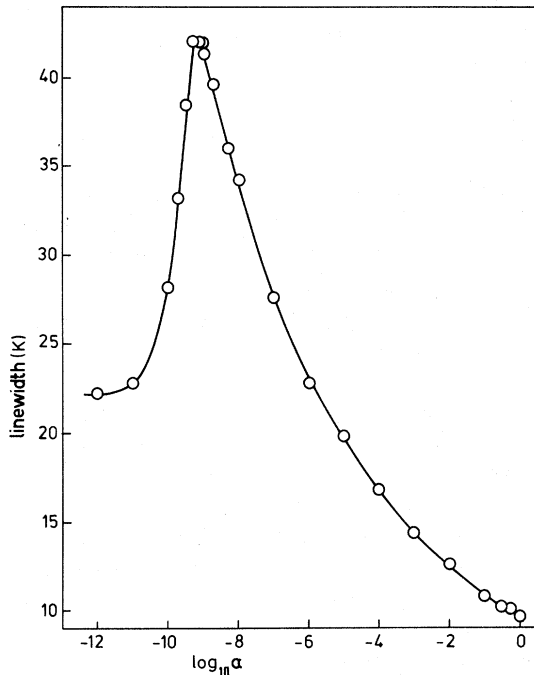


FIG. 8. Calculated HT bandwidth at half height as a function of  $\log_{10}\alpha$ . The same parameters as in Fig. 7 have been used.

For low  $\text{NdF}_3$  concentrations the dissociation constant is about  $2 \times 10^{-8}$ , corresponding with a dissociation energy of 0.4–0.5 eV.

If we are dealing with concentrations larger than a few mol % the overlap between the dipole systems becomes more and more important; therefore, it is no longer possible to treat the dipoles in terms of the above described dissociation model. In Fig. 8 we see that the width of the ITC curves is constant for very small values of  $\alpha$ ; for values above  $10^{-11}$  the width increases and reaches a maximum value for  $\alpha = 10^{-9}$ ; for  $\alpha > 10^{-9}$  the width of the ITC peak decreases with increasing  $\alpha$ . From the comparison between the experimental curve (Fig. 4) and the theoretical one (Fig. 8) we conclude that the model proposed by den Hartog and Langevoort<sup>27</sup> to describe the relaxation mechanism for the space charges in  $R^{3+}$ -doped alkaline-earth fluorides also works reasonably well for crystals with NN dipoles. Characteristic for both Figs. 4 and 8 is the maximum of the bandwidth of the ITC curves; the correction factor to be applied to  $x$  in order to obtain  $\alpha$  in the low-concentration range is about  $10^{-7}$ , i.e., the same as the one obtained from the curves showing the behavior of  $T_{\text{max}}$  vs  $\log_x$  or  $\log_{10}\alpha$ . One should be careful if one wants to compare the absolute values of the ITC bandwidths, because we know from experimental results obtained by van Weperen *et al.*<sup>9</sup> that defect-defect interactions may give a significant contribution to the width of the depolarization peaks. A similar effect is expected to occur for conduction peaks such as the HT band. The broadening will increase with increasing defect concentration; for the system  $\text{SrF}_2:\text{Nd}$  the most important results for the HT band are observed for  $x > 10^{-2}$ , implying that the defect-defect interactions will modify the results appreciably. The broadening, however, is expected to vary rather gradually as a function of the concentration of  $\text{Nd}^{3+}$  impurities. Therefore, the general trend of the width of the ITC band also increases gradually with increasing concentration. If we compare Figs. 3 and 7 we see that the shapes of the lines displaying  $T_{\text{max}}$  as a function of  $\log_{10}x$  or  $\log_{10}\alpha$  are different. To get the same shapes we have to correct the values of  $x$ . For concentrations up to about 5 mol % we see that the ratio between  $x$  and  $\alpha$  is about  $10^{-7}$ . Up to this concentration (or  $\alpha \cong 10^{-8}$ ) both curves have the same shape. It should be noted here that above 5 mol % the individual defects will be very close to each other (we assume for simplicity that there is no clustering). If we are allowed to describe the dipole system sta-



tistically, we can calculate the probability of finding two dipoles very close to each other. We choose a central position for an Nd impurity which has been compensated locally by an NN interstitial  $F^-$  ion. From the crystal structure it is easy to see that this position is surrounded by about 30  $Sr^{2+}$  sites, which can be occupied by another Nd impurity of an NN dipole. These dipoles are so close that the interstitial fluoride ion can jump from one dipole system to the other. In this case it is no longer necessary for the  $Nd^{3+}-F_i^-$  dipoles to dissociate in order to contribute to dc phenomena. Thus, the "effective-dissociation" constant that should be taken into account increases very rapidly for dipole concentrations higher than 5 mol %.

To match Figs. 3 and 7 completely we have to take variable values for the correction factor. We see that this correction factor increases very rapidly with growing concentration. Applying the same correction factors to the plot of the linewidth as a function of  $\log_{10}\alpha$ , the corrected form of Fig. 8 and the experimental plot (Fig. 4) look alike but do not match. For an explanation we probably have to take into account gradients in the  $NdF_3$  concentration within the samples. In these samples the peak position is approximately the same as in a completely homogeneous sample. Only the linewidth will be affected in a rigorous way. Another reason for the deviation may be the broadening of activation energies as treated by van Weperen *et al.*<sup>10</sup>. The calculations carried out in order to obtain the plot of the linewidth as a function of  $\log_{10}\alpha$  employ unique values of the activation energies. So the linewidth plot is only to be used as a qualitative proof for our model for the relaxation of space charges.

## V. DISCUSSION

In Sec. III we have given the theoretical description of the conduction processes in the materials investigated in this paper. The comparison between theory and experiment has shown that the model works reasonably well also for the system  $SrF_2:Nd$ , where one is dealing with rather small dipoles. We have observed that, as expected for small dipoles, one needs relatively high defect concentrations in order to find percolation-type conduction, for which the theoretical formula has been given in Eq. (1). In Fig. 9 we have presented a plot of the percolation effect of the ionic conduction in heavily doped materials. The experimental

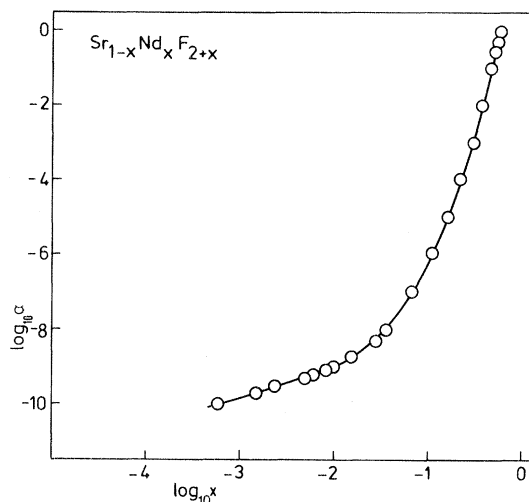


FIG. 9. Values of  $\log_{10}\alpha$  plotted as a function of  $\log_{10}x$  obtained by comparing the experimental Fig. 3 with the theoretical Fig. 7.

plot has been compared with the curve

$$\alpha = A(x - 0.15)^2, \quad (5)$$

and it appears that the experimental curve behaves in accordance with an exponent larger than 2. We should realize however, that there are some problems with the determination of  $\alpha$ . Firstly, the error bars connected with the experimental points in Fig. 3 are rather large. Secondly, for heavily doped materials the lattice parameter will deviate from that of pure  $SrF_2$ ; this may lead to a change in the position of the HT band resulting in an error of the values of  $\alpha$ . The latter effect is expected to be relatively unimportant for the system  $BaF_2:La$ , because the estimated value for the critical concentration  $x_c$  is 2.2 mol %, whereas for the system  $SrF_2:Nd$  it is between 10 and 15 mol %.

Experiments carried out earlier in this laboratory indicated that for moderate concentrations of trivalent impurities the ITC peaks associated with dipole reorientation are broadened appreciable. Similar effects are expected to occur for space-charge peaks, such as the HT band. In principle it is possible to describe the shape of the HT band, taking into account that the activation energies associated with the relaxation mechanisms indicated in Eq. (3) do not have a unique value. We have not carried out this analysis because there are seven parameters which should be fitted:  $\tau_0^f$ ,  $E_0^f$ ,  $p_f$ ,  $\tau_0^d$ ,  $E_0^d$ ,  $p_d$ , and  $C$ . These parameters are the characteristic relaxation time for jumps of free interstitials, the mean activation energy of free interstitials, the width of the distribution function describ-

ing the distribution of activation energies of the jumps of free interstitials, the characteristic relaxation time of dipole jumps, the mean activation energy of dipole jumps, the width of the distribution of activation energies associated with dipole jumps, and the integrated depolarization current (total charge), respectively. We have shown that the accuracy of the broadening parameter as derived from a simple dipole-depolarization peak is rather poor (see van Weperen *et al.*<sup>9</sup>). It is expected that for the analysis of the space-charge peaks the situation is far worse. It should be noted, however, that the broadening parameters  $p_f$  and  $p_d$  will influence both the position and the width of the HT band. Therefore, this effect will also reduce the accuracy of the results obtained from the model that has been employed in this paper.

From the observed behavior of the position of the HT band and the width of this band we conclude that extensive clustering of  $\text{Nd}^{3+}\text{-F}_i^-$  dipoles in  $\text{SrF}_2$  is not very likely. This conclusion is supported by the EPR results on crystals which had been doped with  $\text{Nd}^{3+}$  and traces of  $\text{Gd}^{3+}$ . The

$\text{Gd}^{3+}$  ions are located at cubic sites in these materials, and even for  $\text{Nd}^{3+}$  concentrations up to 6 mol % no extensive clustering, in which the Gd impurities are involved, has been observed. We only found a gradually increasing broadening of the EPR lines of  $\text{Gd}^{3+}$  due to increased interactions between the central  $\text{Gd}^{3+}$  ions and the surrounding defects, which have been distributed predominantly statistically over the positions available.

#### ACKNOWLEDGMENTS

The authors wish to thank Mr. P. Wesseling, Mr. R. P. Flanderijn, and Mr. J. F. M. Wieland for growing crystals, technical assistance, and making drawings, respectively. This work is part of the research program of the "Stichting Fundamenteel Onderzoek der Materie" and has been made possible by financial support from the "Nederlandse Organisatie voor Zuiver Wetenschappelijk Onderzoek."

- <sup>1</sup>W. Bollman, P. Görlich, W. Hauk, and H. Mothers, *Phys. Status Solidi A* **2**, 157 (1970).
- <sup>2</sup>W. Bollman, *Phys. Status Solidi A* **18**, 313 (1973).
- <sup>3</sup>P. D. Southgate, *J. Phys. Chem. Solids* **27**, 1623 (1966).
- <sup>4</sup>A. D. Franklin and S. Marzullo, *J. Phys. C* **3**, L171 (1970).
- <sup>5</sup>A. Edgar and H. K. Welsh, *J. Phys. C* **8**, L336 (1975).
- <sup>6</sup>A. Edgar and H. K. Welsh, *J. Phys. C* **12**, 703 (1979).
- <sup>7</sup>E. L. Kitts Jr., M. Ikeya, and J. H. Crawford Jr., *Phys. Rev. B* **8**, 5840 (1973).
- <sup>8</sup>B. P. M. Lenting, J. A. J. Numan, E. J. Bijvank, and H. W. den Hartog, *Phys. Rev. B* **14**, 1811 (1976).
- <sup>9</sup>W. van Weperen, B. P. M. Lenting, E. J. Bijvank, and H. W. den Hartog, *Phys. Rev. B* **16**, 2164 (1977).
- <sup>10</sup>W. van Weperen and H. W. den Hartog, *Phys. Rev. B* **18**, 2857 (1978).
- <sup>11</sup>P. W. M. Jacobs and S. H. Ong, *J. Phys. Chem. Solids* **41**, 431 (1980).
- <sup>12</sup>S. H. Ong and P. W. M. Jacobs, *J. Solid State Chem.* **32**, 193 (1980).
- <sup>13</sup>E. Laredo, M. Puma, N. Suarez, and D. R. Figueroa, *Phys. Rev. B* **23**, 3009 (1981).
- <sup>14</sup>G. E. Matthews Jr., B. J. Faraday, N. D. Wilsey, and J. H. Crawford Jr., *Phys. Rev. B* **23**, 5011 (1981).
- <sup>15</sup>S. H. N. Wei and D. C. Ailion, *Phys. Rev. B* **19**, 4470 (1979).
- <sup>16</sup>A. Kiel and W. B. Mims, *Phys. Rev. B* **6**, 34 (1972).
- <sup>17</sup>L. A. Boatner and R. W. Reynolds, *J. Chem. Phys.* **52**, 1248 (1970).
- <sup>18</sup>Chi Chung Yang, Sook Lee, and Albert J. Bevolo, *Phys. Rev. B* **13**, 2762 (1976).
- <sup>19</sup>J. M. Baker, E. R. Davies, and T. R. Reddy, *Contemp. Phys.* **13**, 45 (1972).
- <sup>20</sup>C. Bucci, R. Fieschi, and G. Guidi, *Phys. Rev.* **148**, 816 (1966).
- <sup>21</sup>A. B. Aalbers and H. W. den Hartog, *Phys. Rev. B* **19**, 2163 (1979).
- <sup>22</sup>D. R. Tallant and J. C. Wright, *J. Chem. Phys.* **63**, 2074 (1975).
- <sup>23</sup>J. J. Fontanella and C. Andeen, *J. Phys. C* **9**, 1055 (1976).
- <sup>24</sup>D. R. Tallant, D. S. Moore, and J. C. Wright, *J. Chem. Phys.* **67**, 2897 (1977).
- <sup>25</sup>C. G. Andeen, J. J. Fontanella, M. C. Wintersgill, P. J. Welcher, R. J. Kimble, Jr., and G. E. Matthews, Jr., *J. Phys. C* **14**, 3557 (1981).
- <sup>26</sup>Z. C. Nauta-Leeffers and H. W. den Hartog, *Phys. Rev. B* **19**, 4162 (1979).
- <sup>27</sup>H. W. den Hartog and J. C. Langevoort, *Phys. Rev. B* **24**, 3547 (1981).
- <sup>28</sup>S. Kirkpatrick, *Rev. Mod. Phys.* **45**, 574 (1973).
- <sup>29</sup>E. J. Bijvank, A. G. Zandbergen-Beishuizen, and H. W. den Hartog, *Solid State Commun.* **32**, 239 (1979).
- <sup>30</sup>G. K. Miner, T. P. Graham, and G. T. Johnston, *J. Chem. Phys.* **57**, 1263 (1972).
- <sup>31</sup>M. V. Vlasova, N. G. Kakazei, and L. A. Sorin, *Kristallografiya* **19**, 395 (1974) [*Sov. Phys.—Crystallogr.* **19**, 243 (1974)].
- <sup>32</sup>E. J. Bijvank, H. W. den Hartog, and J. Andriessen, *Phys. Rev. B* **16**, 1008 (1977).
- <sup>33</sup>H. W. den Hartog and R. van der Meulen (unpublished).